ground water

# Field Test of the Superconducting Gravimeter as a Hydrologic Sensor

by Clark R. Wilson[1], Bridget Scanlon[2], John Sharp[2], Laurent Longuevergne[2], and Hongqiu Wu[2]

## Abstract

We report on a field test of a transportable version of a superconducting gravimeter (SG) intended for groundwater storage monitoring. The test was conducted over a 6-month period at a site adjacent to a well in the recharge zone of the karstic Edwards Aquifer, a major groundwater resource in central Texas. The purpose of the study was to assess requirements for unattended operation of the SG in a field setting and to obtain a gravimetric estimate of aquifer specific yield. The experiment confirmed successful operation of the SG, but water level changes were small (<0.3 m) leading to uncertainty in the estimate of specific yield. Barometric pressure changes were the dominant cause of both water level variations and non-tidal gravity changes. The specific yield estimate (0.26) is larger than most published values and dependent mainly on low frequency variations in residual gravity and water level time series.

## Introduction

This paper reports on a field test of a transportable superconducting gravimeter (SG) designed to monitor surface gravity and provide a direct measure of water storage change in the subsurface. There has been growing interest in monitoring subsurface fluid storage changes with gravity, and published studies have employed portable gravimeters of either relative (proof mass-on-spring) or absolute (free-falling mass) designs. Measurement precision of these gravimeters is in the range of 20 to 150 nm/s$^2$. Examples include monitoring of groundwater by Pool and Eychaner (1995), Naujoks et al. (2007), and Gehman et al. (2009), and of petroleum by Ferguson et al. (2007). [The SI unit of acceleration (nm/s$^2$) is equivalent to 0.1 μGals in traditional geophysical units of Galileos (Gals or cm/s$^2$).]

The SG is distinguished from other gravimeters by superior precision, better than 1 nm/s$^2$ and by the ability to record gravity continuously over periods of months and longer. The SG is a relative gravimeter (Prothero and Goodkind 1968) employing a hollow niobium 0.0254 m spherical proof mass, with magnetic fields replacing the metal or quartz spring of a conventional relative gravimeter. Proof mass and surrounding coils are maintained in a superconducting state by a liquid helium bath. Like all relative gravimeters, the SG requires calibration to convert its output (voltage) to units of nm/s$^2$, and is accomplished here by comparing the SG tidal signal with predicted Earth tides. A full discussion of SG principles, development history, performance, and data analysis is given by Goodkind (1999). Hinderer et al. (2007) summarize geophysical applications and many other aspects, including an analysis of SG precision.

The disadvantage of the SG has been its cumbersome size. Prior to construction of the instrument used in this study, all SG's (more than 30 world wide) have been permanently installed in observatories (Crossley et al. 1999). Growing interest in hydrologic applications of gravity motivated the development of a transportable version (Wilson et al. 2011), which involved packaging a standard observatory instrument into two enclosures (each weighing about 200 kg), developing procedures for transport, setup and operation, and testing the system in a variety of environments. Here we describe a 6-month test

[1]Corresponding author: Jackson School of Geosciences, University of Texas Austin, Austin, TX 78712; crwilson@jsg.utexas.edu
[2]Jackson School of Geosciences, University of Texas Austin, Austin, TX 78712.

Received April 2011, accepted July 2011.

doi: 10.1111/j.1745-6584.2011.00864.x

(November 2008 to June 2009) at an unattended field site in the recharge zone of the Edwards Aquifer of Central Texas. The experimental goals were to assess operational requirements and capabilities of the SG in a field setting and to obtain a gravimetric estimate of aquifer specific yield $S_y$.

## Experimental Setting

The experiment was conducted in the Barton Springs Portion of the karstic Edwards Aquifer (Figure 1), a major regional water resource in Central Texas and the principal water supply for the city of San Antonio. There is an extensive groundwater monitoring network in the region (Smith and Hunt 2004), and dye tracer tests show horizontal flow velocities up to 12 km/d (Smith et al. 2005). Recharge occurs primarily from surface flow directly to the water table through sinkholes and other vertical conduits, and during periods of heavy rain, water levels in monitoring wells may increase by several meters over periods of days to weeks. We anticipated that one or more recharge events would be observed during the experiment, which included the spring season when heavy thunderstorms are common. The goal was to use simultaneous measurements of water level and gravity change to show how aquifer storage (in caves, tunnels, fractures, and the limestone matrix) responds to transient inputs.

The experiment was conducted at well 58-49-940 (Figure 1), drilled in the 1970s to provide water for a cattle ranch. The ranch was acquired in the late 1990s by the City of Austin to preserve Edwards Aquifer recharge areas. The well is reported to be open to its full depth, with the exception of a steel casing near the surface.

Figure 2 summarizes general stratigraphy at the study site, and relationships to well depth and sensor location. A more complete description of stratigraphy is given by Rose (1972). Formation descriptions are derived mainly from exposed outcrops west of the Balcones Fault, corresponding approximately to the western edge of the recharge zone in Figure 1. At the experiment site, the surface unit is the 10-m thick Grainstone member of the Kainer Formation, where erosion has left at most a few meters. Below this are the 20-m Kirschberg member, the 40-m Dolomitic member, and the 15-m basal Walnut member. Beneath this, the Upper Glen Rose Limestone forms the Upper Trinity Aquifer, generally considered to be confined by the Walnut member. The Kirschberg is a cave forming unit with high porosity and numerous voids where exposed, but is well above the water table during the experiment. The Dolomitic member has less porosity and less evidence of void interconnectivity when seen in outcrop. The underlying Glen Rose Limestone has few solution features in the Austin Area, probably due to beds of marl that limit water circulation.

Site instrumentation consisted of the SG and a Paroscientific Met-3 barometer mounted in the instrument shed (Figure 3); a separate weather station with soil moisture probes; and an in situ Level Troll 500 water

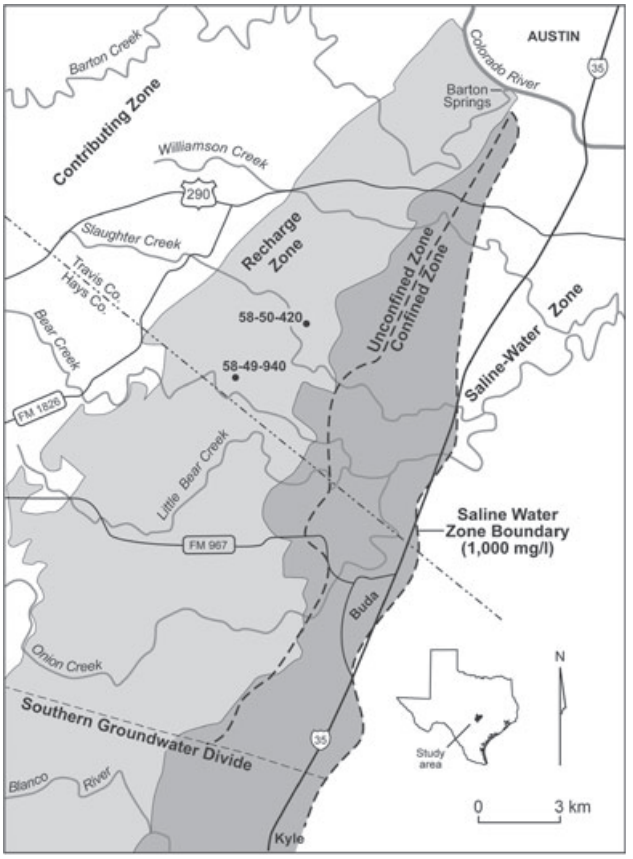


**Figure 1. Barton Springs Portion of the Edwards Aquifer after Hunt et al. (2004). The experiment was conducted at well 58-49-940. A new period of SG observations began at well 58-50-420 in March 2011.**

level sensor (30 psi) with vented cable mounted in the well. A gravimeter monument was constructed of 25 mm threaded steel rods cemented into holes drilled into outcropping limestone to a depth of about 0.7 m. A plywood floor supported by separate cemented rods supported the gravimeter shed. As discussed below, two gaps in the data are attributed to problems with the gravimeter monument and plywood floor. A concrete slab is the preferred monument design, but was not permitted by City of Austin site regulations.

The SG and barometer were sampled at 1 Hz with global positioning system (GPS) timing control, and subsequently decimated to 15-min samples. Water level was sampled every 15 min, with timing controlled by the Level Troll 500 internal clock, which can drift up to 1 s/d. Manufacturers' specifications give water level precision as better than 1 mm and better than 0.1 mbar (1 Pa) for barometric pressure.

## Interpretation of Surface Gravity Changes

A gravimetric estimate of $S_y$ is useful in a karst setting because it is a spatial average over dimensions much larger than scales of typical heterogeneities such as caves, fractures, and tunnels. Assuming that stored water is added or removed at the water table, the vertical

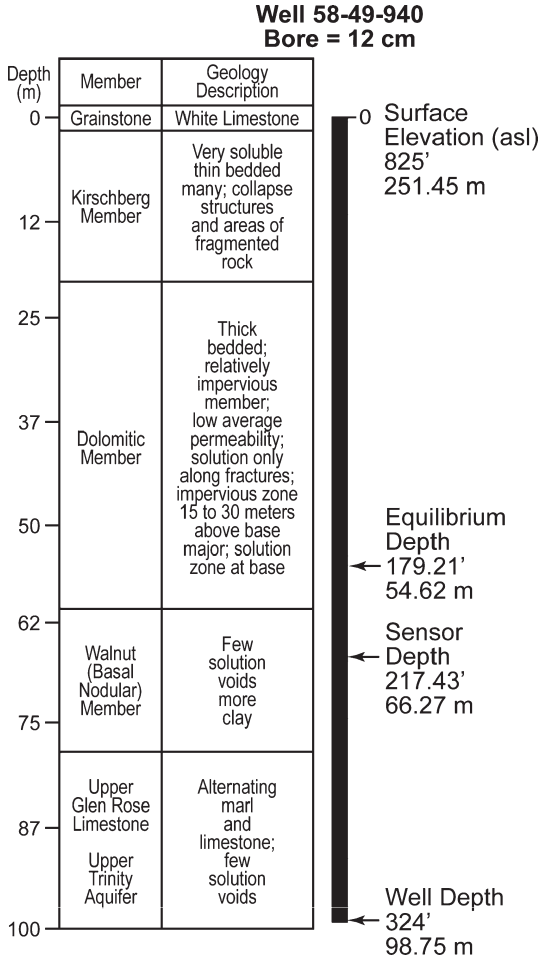


**Figure 2. Generalized stratigraphy of the Edwards Aquifer, Barton Springs Segment, with approximate well dimensions. Equilibrium depth corresponds to average water depth during the experiment.**

averaging scale is set by the range of water level variations observed in an experiment. We adopt the convention that the horizontal averaging scale (the "footprint") is approximately 20 times depth to the water table, a region that accounts for about 90% of the gravity change, as illustrated in Figure 4. If an uniform water layer of infinite horizontal extent, thickness $\Delta h$, and density $\rho$ is added to the water table at depth $Z$, the Bouguer infinite slab formula (Pool 2008) predicts that gravity will increase by $(2\pi\rho G\Delta h)$, where $G$ is the gravitational constant. The central circular disk of diameter 20 Z accounts for 90% of this. In this study, $Z$ is near 54 m (Figure 2) so the assumed footprint is about 1 km. In some situations (a much shallower water table or significant lateral variations in water table depth), the spatial footprint of a surface gravity measurement at a single point may be smaller than desired. In such cases, a high precision measurement of gravity change at a single surface point might be combined with repeated lower precision portable gravimeter observations in surrounding areas. An example of this approach is the study of Jacob et al. (2010).

Substituting values for water density and $G$ into the Bouguer formula, gravity changes by 419.2 nm/s$^2$ per

**Figure 3. The SG is shown within the gravimeter enclosure inside the instrument shed. The enclosure door is open, showing the liquid helium dewar on the left and rack-mounted instruments on the right. The cryogenic refrigeration and power supply enclosure is behind the shed and not visible. Electricity consumption of about 2 kW (mainly for the cryogenic refrigerator) requires a wired power source rather than solar panels. Data communication was by wireless modem.**

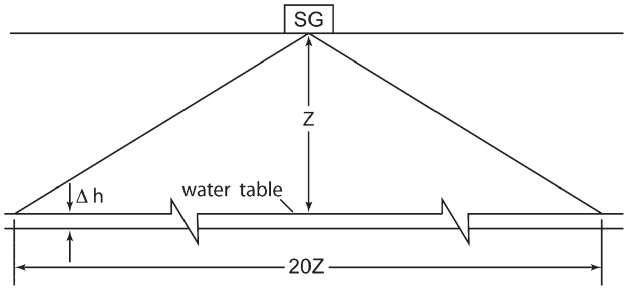


**Figure 4. Geometry of gravity change at the surface in terms of a uniform layer of water of thickness $\Delta h$ added at a horizontal water table at depth $Z$; 90% of the gravity change measured by the SG at the surface is due to a circular disk of diameter 20$Z$. The remaining 10% comes from the region outside the disk, which extends to infinity.**

meter of water. With precision exceeding 1 nm/s$^2$ the SG is able to detect storage changes equivalent to a 2-mm water layer, whereas other types of gravimeters would be unable to detect storage changes unless they exceeded the equivalent of about a 40-mm water layer.

In terms of aquifer properties, if gravity changes at the surface by $\Delta g$ and water level changes in the aquifer by $\Delta h$, then $S_y$ is related to these by

$$\Delta g = 419.2\ S_y \Delta h \text{ or } S_y = (1/419.2)[\Delta g/\Delta h] \quad (1)$$

In addition to aquifer storage effects, a gravimeter fixed to the surface measures changes due to other causes. Earth tide and barometric pressure contributions are discussed in detail below. Soil moisture storage changes may also contribute to the gravity signal, although in this study, their effect was negligible due to drought conditions. An additional contribution may arise from vertical

site displacement within Earth's field gradient (Free Air Gradient, 3 nm/s$^2$ decrease per mm of elevation increase). In this study, we assumed that vertical motion effects are negligible given the location on outcropping limestone. However, in some applications, surface displacements might be significant and correlated with soil moisture or aquifer storage changes. This would require mm-level vertical control via GPS.

## Experimental Results

Data include 15-min samples of water level in the well, gravity change, barometric pressure, and various weather variables such as soil moisture, wind, precipitation, and others, for 186 d beginning November 1, 2008. We measure time in days beginning on this date. The experiment coincided with the most severe drought in Central Texas since the 1950s. Prior to Day 126, only three precipitation events, with daily totals in the range of 5 to 12 mm, were observed. On Day 126, a 45-mm rainfall caused the gravimeter monument to shift beyond the limit of the SG tilt compensation system. The result was a gap in the gravity time series of almost 3 weeks. This was in addition to an earlier data gap starting around Day 10 due to a sagging plywood floor in the instrument shed. The longest continuous portion of the gravity series extends from Days 25 to 125. Measured soil moisture was approximately zero, except for small increases that persisted for a few days after the precipitation events.

A gravimetric estimate of $S_y$ is derived by comparing time series of gravity and water level after processing to remove unrelated variations. The software package Tsoft (Van Camp and Vauterin 2005) is designed for many of the required tasks and we have used it in combination with MATLAB.

The data processing steps required to use the SG as a hydrologic sensor are described below, but before reviewing these we show why it is essential to remove barometric pressure effects from both water level and gravity time series. Surface gravity will change with barometric pressure due to variable Newtonian attraction of the atmosphere above the gravimeter. The Bouguer infinite slab formula predicts change by an amount $\alpha = -4.19$ nm/s$^2$ per mbar pressure increase. As a result of load deformation, topography, and seasonally variable barometric pressure spatial scales, estimates of $\alpha$ from actual SG data fall in the range $-2$ to $-3.5$ nm/s$^2$ (Crossley et al. 1995). Water level in a well may also respond to barometric forcing, an effect described by barometric efficiency $\beta$, the ratio of water level decrease due to barometric pressure increase. $\beta$ is dimensionless if water level change is converted to pressure change. A typical value $\beta = 1$, implies 0.01 m water level decrease per mbar of barometric pressure increase. If there is a barometric pressure increase of 1 mbar (with no change in aquifer storage), both gravity and water level will decrease, just as they would for a change in aquifer storage. For example, for typical values $\beta = 1$ and $\alpha = -3$, a 1 mbar barometric pressure increase will lead to

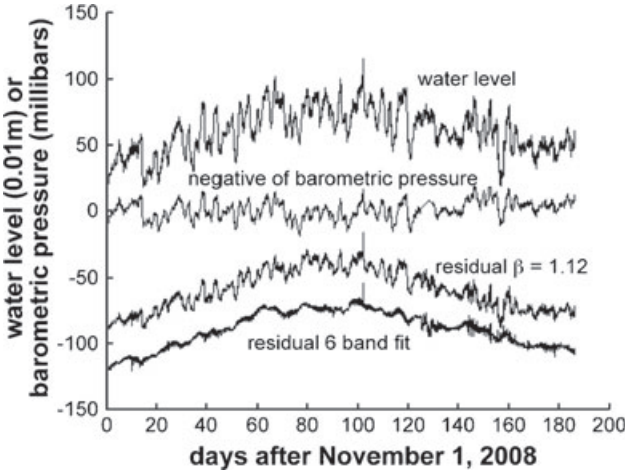


**Figure 5. From top to bottom: water level time series; negative of barometric pressure change; residual water level after subtracting barometric pressure scaled using a single value $\beta = 1.12$; and (bottom) residual water level after fitting six values of $\beta$ in Table 1, and subtracting scaled band-passed barometric pressure series. Mean values have been removed and series are offset for clarity.**

an apparent estimate of $S_y$ of about 0.71 since Equation 1 implies

$$-3 \text{ nm/s}^2 = 419.2\ S_y(-0.01 \text{ m}) \qquad (2)$$

Therefore, barometric pressure effects need to be removed from both gravity and water level series to avoid contaminating the gravimetric estimate of $S_y$.

## Water Level Time Series Processing

Figure 5 shows the water level time series for Days 1 to 186, the negative of barometric pressure changes, and two different residual water level time series, corresponding to two attempts to remove barometric pressure effects. Barometric pressure changes do not show long period changes evident in the water level series with time scales of several months. However, Figure 5 shows that at times scales of a few weeks and less barometric pressure changes appear to be highly (negatively) correlated with water level changes. The first water level residual series in Figure 5 is obtained by removing the barometric pressure series scaled by estimate of $\beta = 1.12$, which is the least-squares estimate using the full barometric pressure and water level time series. Using this single value of $\beta$ leaves a residual that is clearly correlated with barometric pressure. We tried other methods to remove barometric pressure effects, none of which was completely successful. In one reasonably successful approach, we let $\beta$ depend on frequency. Using third order zero-phase Butterworth filters, we separated barometric pressure and water level series into a number of defined frequency bands and estimated separate values of $\beta$ for each band. Then, each band-passed barometric pressure series, scaled by its value of $\beta$, was removed from the water level series. Figure 5 (lower curve) shows

**Table 1**
**Estimates of $\beta$ Derived from Least-Square Fits of Band-Passed Barometric Pressure to Band-Passed Water Level Time Series**

| Period Range | Estimated $\beta$ |
|---|---|
| 20–30 d | 1.35 |
| 10–20 d | 1.69 |
| 5–10 d | 1.89 |
| 2.5–5 d | 2.00 |
| 1.25–2.5 d | 1.96 |
| <1.25 d | 1.90 |

Note: Zero-phase Butterworth band pass filters were used to separate each series into bands corresponding to the indicated period range in days. No barometric pressure effects were removed at periods longer than 30 d.

the residual after removing barometric pressure using six frequency bands. Table 1 shows corresponding estimates of $\beta$ are about 2 at short periods, diminishing at longer periods. This approach seems to remove most of the barometric pressure-related variance from the water level series, but the residual still appears to be related to large, rapid barometric pressure changes. With most barometric contributions removed, the lower residual curve in Figure 5 reveals variations due to tides and a number of short-duration fluctuations which begin to increase in frequency about Day 100. The short-duration variations are probably related to increased spring-time pumping activity at nearby commercial wells. An interpretation of both $\beta$ and tidal variations is given below.

## Gravity Time Series Processing

Earth tide gravity variations are one to two orders of magnitude larger than the expected water storage signal, but are highly predictable and easily removed. In a usual SG data processing sequence, typically performed using the Tsoft package, a theoretical Earth tide time series is fit by least squares and subtracted from the gravity series. This removes about 99% of the tide signal, and provides a calibration factor for the SG. A residual tide is then removed by a least-square fit to sinusoids at major tidal frequencies. These residual tides with amplitudes of 20 to 30 nm/s$^2$, (about 1% of the total tide signal) arise from ocean loading, even at locations distant from the coast.

It is also customary to remove an estimated component of instrument drift. Some amount of drift is observed in virtually all SG records, because of atomic-scale changes in the proof mass and other unknown processes. The rate typically diminishes over time, and an exponential time function is an accepted empirical model. Unfortunately, in this experiment SG drift rate was too large to follow a standard processing sequence. In a laboratory setting prior to the field experiment, the drift rate was nearly 9 nm/s$^2$/d, about 30 times larger than manufacturer GWR's (GWR Instruments, Inc., San Diego, California) specifications. GWR agreed to replace the sensor, but we decided to proceed with the field experiment because City of Austin site permits would otherwise expire. Afterward, repairs reduced the drift rate to within specifications, and we do not anticipate encountering this problem again. However, because drift over 6 months was comparable with the Earth tide signal (~2000 nm/s$^2$), least-square estimates of the two components would influence one another, so tides and drift were removed iteratively. First a theoretical Earth tide (WDD in Tsoft) and linear drift term were fit simultaneously. Then the linear drift was removed from the original series and the tides were fit a second time, also yielding the calibration factor. The second Earth tide estimate was subtracted from the data, and an exponential drift model was fit to the residual.

The remaining step is to remove barometric pressure effects. We used different segments to estimate $\alpha$ and found reasonably good results using Days 50 to 80 when the gravity series was relatively free of high frequency noise (Figure 6). The upper curve (gravity) and the middle curve (negative of barometric pressure change) are strongly correlated, and the estimate ($\alpha = -3.38$) is a typical value (Crossley et al. 1995). However, seasonal variability is possible, so barometric effects may not be completely removed using a single $\alpha$ for the entire series.

## Gravimetric Estimate of $S_y$

Figure 7 shows final residual gravity and water level time series. With the exception of the segment for Days 1 to 9, low frequency variations in gravity and water level appear correlated. For Days 1 to 9 the gravity series was affected by the sagging plywood floor in the instrument shed, and is excluded from further analysis. The two remaining segments of the gravity series show high frequency variations, changing in character over time. These may be due to weather-related vibration, instability

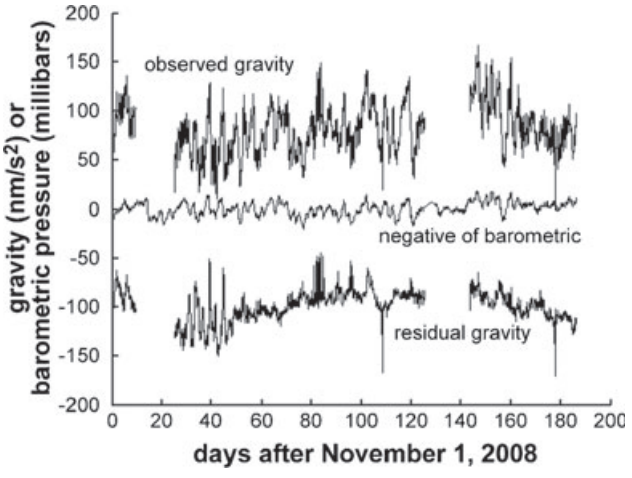


**Figure 6. Gravity time series: residual after removing theoretical tides and drift (upper); negative of barometric pressure (middle); and residual after removing residual ocean load tides and barometric pressure effects with $\alpha = -3.38$ determined from Days 50 to 80.**

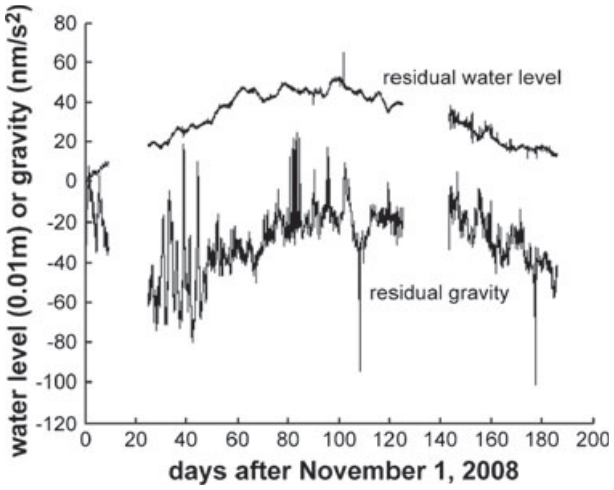


**Figure 7. Residual gravity (lower) and water level time series (upper). Relative to Figure 5, the water level residual has had diurnal and semidiurnal tidal variations removed. Series are offset for clarity.**

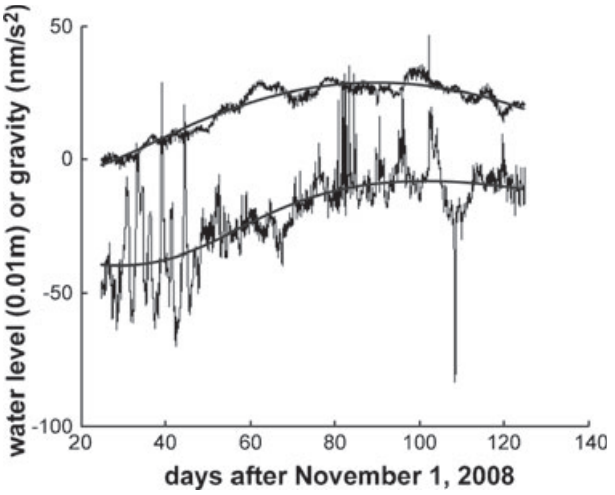


**Figure 8. Residual gravity (lower curve) and water level (upper) for Days 25 to 125 shown with quartic polynomials fit by least squares. Series have zero mean but are offset for clarity.**

**Table 2**
**Estimates of $\gamma$ from the Second and Third Series Segments in Figure 7**

| Segment | $\gamma$ (Full Series) | $\gamma$ (Polynomial Fit) | $S_y$ |
|---|---|---|---|
| Days 25–125 | 107 | 121 | 0.26 |
| Days 144–186 | 159 | 175 | 0.38 |

Notes: Estimates of $\gamma$ are determined by a least-square regression as described in the text, either using the full series or the polynomial fit to it. The estimate of $S_y$ corresponds to $\gamma$ from the full series, and the origin of the confidence interval is described in the text.

in the monument, nearby road construction noise, residual barometric pressure effects, and other sources. There is no evidence that they are related to water storage changes.

From Equation 1, with water level changes $\Delta h$ given in meters and gravity change $\Delta g$ in nm/s$^2$, a gravimetric estimate of $S_y$ is proportional to the ratio $[\Delta g/\Delta h]$, which is estimated from the two longer portions of the gravity series, Days 25 to 125 and Days 144 to 186. After removing the mean of each time series segment we find the coefficient $[\gamma]$ which is the least-squares solution to $\gamma \Delta h = \Delta g$ where $\Delta h$ and $\Delta g$ are residual time series in Figure 7. The estimate of $S_y$ from Equation 1 is then $\gamma/(419.2)$. Table 2 gives estimates $S_y = 0.26$ from Days 25 to 125 and 0.38 from Days 144 to 186. We also estimate $\gamma$ by fitting low order polynomials to each by least squares, and then estimate $\gamma$ from the polynomials in place of the residual series. This is a simple way to remove short period variations in gravity and water level residuals that are unlikely to be related to aquifer storage changes. In addition, contamination from residual barometric pressure effects will be minimized because Figures 5 or 6 show that the barometric series lacks similar long period variations. Figure 8 shows an example, in which quartic polynomials have been fit for Days 25 to 125. For Days 144 to 186, we used a quadratic polynomial that is not shown.

It is difficult to assess confidence in the gravimetric estimates of $S_y$, given that they are derived from a long period signal of small magnitude in each series. A qualitative sense of confidence comes from the physically possible range of estimates, and visual evidence for correlation at long periods (Figures 7 and 8). Long period correlation also suggests that data processing steps required to obtain the gravity residual, especially drift removal, have not corrupted the residual low frequency gravity signal. We take as an approximate measure of uncertainty differences between estimates derived from time series and from the quartic polynomials. Differences are about 13%, so we suggest this as a measure of uncertainty in estimates of $S_y$. In addition to this, we conducted a Monte-Carlo experiment to estimate confidence intervals. We let the gravity polynomial (Figure 8) represent the true signal, and modeled short period variations (misfits to the polynomials in Figure 8) as Gaussian white noise, with standard deviations from residuals in Figure 8. This yields a 90% confidence interval 2% on either side of the estimate. This is likely an underestimate of uncertainty, because deviations from the polynomials are neither white nor stationary.

## Discussion

The recharge zone would normally be considered an unconfined part of the Edwards Aquifer. In unconfined clastic aquifers, both barometric efficiency and tidal variations in water level are expected to be nearly zero, so the observed high barometric efficiency and tidal response both require some explanation. Diurnal and semidiurnal tidal variations in water level have peak-to-peak variations of about 0.04 m, and are just visible in the lower residual curve in Figure 5 after most of barometric pressure effects have been removed. Rojstaczer

and Agnew (1989, Figure 2) show that tidal variations of this magnitude would be expected in a well penetrating a confined limestone aquifer with porosity near 10%. Figure 2 suggests that well 58-49-940 may penetrate the confined Upper Trinity Aquifer, so a straightforward explanation is that tidal variations in water level reflect Trinity rather than Edwards Aquifer response. In contrast, the large magnitude of $\beta$ and its variability with frequency (Table 1) are more difficult to explain. Because linear least-squares was not completely effective in removing barometric effects, there is also an indication that the response may not be linear.

We present a qualitative explanation for the large barometric efficiency and its frequency dependence which may have some relevance to estimated values of $S_y$. A quantitative analysis is beyond the scope of this study. Our hypothesis is that the observed $\beta$ represents the superposition of two effects. One is the response of a confined aquifer, for which $\beta = 1$ (Batu 1998). Although the recharge zone is nominally unconfined, it appears that the karst aquifer shows confined behavior within the region sampled by the well. The second effect, which adds to this, is proposed to be due to ubiquitous air-filled cavities at and near the water table, leading to high effective compressibility of the fluid responding to barometric pressure forcing. Compressibility of a combination of water and air is the sum of their separate compressibilities scaled by volume fraction of each (Fredlund 1976). If the responding fluid is dominantly air, it will be highly compressible, causing water level in the well to decrease about 0.01 m per mbar of barometric pressure increase as the responding fluid compresses. The sum of the two effects would then make the observed value of $\beta$ double that of a confined aquifer. To explain the frequency dependence of $\beta$, suppose the air-filled cavities near the water table are sealed at short periods but equilibrate with surface barometric pressure at longer periods. Then at longer periods the fraction of air in the responding fluid will diminish as the cavities equilibrate with surface barometric pressure, so the compressibility effect will diminish, and $\beta$ will approach 1.

The smallest gravimetric estimate of $S_y$ derived in this experiment (0.26 or 26%) is similar to the average porosity of the Edwards Aquifer in the San Antonio segment, which is 21.7% (Hovorka et al. 1993), but is larger than published estimates of $S_y$ derived from numerical models or well hydrographs. Numerical model estimates are parameters adjusted to match model output to observed spring-flow discharge. Models do not directly simulate flow in aquifer fractures or conduits, and estimates one or two orders of magnitude lower than ours are typical (e.g. $10^{-2}$, Scanlon et al. 2003; $2 \times 10^{-3}$ to $5 \times 10^{-3}$, Smith et al. 2004). These numerical model parameters tend to be similar to estimates from well response data (e.g. $10^{-3}$ to $2.3 \times 10^{-2}$, Senger and Kreitler 1984; $2.6 \times 10^{-4}$, Hovorka et al. 1998), which perhaps better represent fracture and conduit properties but not long-term specific yield. We consider the gravimetric estimates to be plausible considering they represent a horizontal average of 1 km or more, but a vertical average over less than one-half meter (the observed range of water level fluctuations). Large values of $S_y$ might be expected in zones of concentrated limestone dissolution, and the qualitative explanation of the observed behavior of $\beta$ (air-filled cavities near the water table) suggests that our experiment samples such a zone. Differences in estimates of $S_y$ for the two portions (Days 25 to 125 and Days 144 to 186) might be related to slight differences in mean water level (hence the sampled vertical interval) for these two periods of time.

## Conclusions

Due to drought conditions, storage-related gravity changes were only about 30 nm/s$^2$ (3μGals) over several months, at or below the precision achievable with portable absolute or relative gravimeters. The SG has been able to observe groundwater signals of this magnitude over similar time scales in observatory settings (Kroner and Jahr 2006; Boy and Hinderer 2006; Van Camp et al. 2006), so an important conclusion is that comparable results are possible in a field setting. In more normal (non-drought) conditions, occasional high precipitation events would be expected to create gravity signals about an order of magnitude larger, measurable by both the SG as well as conventional gravimeters. Under these conditions, the time required to obtain useful hydrologic measurements with the SG might be much less than 6 months.

Following earlier reports on the development of a transportable SG (Wilson et al. 2007, 2008), growing interest in the SG as a possible hydrologic instrument led GWR to develop a much more portable version, the iGrav. The first iGrav was delivered in early 2011. The new design, with mass below 30 kg (excluding the cryogenic refrigerator), greatly reduces difficulties in transporting the instrument between sites, and makes it unlikely that the effort to adapt a standard observatory SG (Wilson et al. 2011) will be repeated. However, whether the iGrav or a standard SG is used, a similar experimental setup will be required. This study verified that unattended field operation is feasible, but showed the importance of a stable monument (e.g. a concrete slab), in addition to other necessities of wired electric power to operate the cryogenic refrigerator, and climate control for the refrigerator and electronic components.

A final matter is to assess the future role of the SG as a tool in obtaining gravimetric estimates of groundwater storage changes and aquifer parameters. SG advantages include uniquely high precision and ability to observe and record gravity changes over many time scales. Disadvantages include restricted mobility and possible contamination of signal by instrument drift. Without constraining drift in some manner, the SG, by itself, would probably not be useful in monitoring aquifer storage changes. SG drift can be independently determined via periodic side-by-side observations with an absolute gravimeter, or, as in this study, using correlated water level changes to show that the empirical drift estimate

is reasonable. Limitations of its restricted mobility (and finite spatial footprint) can be overcome using additional observations with portable gravimeters, if the signal is sufficiently large. Because the capabilities of the SG are complementary to other instruments, the greatest promise for hydrologic applications appears to be studies which employ it in combination with other gravimeter types.

## Acknowledgments

This study was supported by the National Science Foundation under grant EAR03-45864. Additional support was provided by the Geology Foundation of the Jackson School of Geosciences, University of Texas. We appreciate significant assistance and cooperation from Brian Hunt and Brian Smith of the Barton Springs Edwards Aquifer Conservation District and Kevin Thuesen of the Water Utility Office of the City of Austin.

## References

Batu, V. 1998. *Aquifer Hydraulics*. New York: John Wiley & Sons Inc.

Boy, J.-P., and J. Hinderer. 2006. Study of the seasonal gravity signal in superconducting gravimeter data. *Journal of Geodynamics* 41: 227–233.

Crossley, D., J. Hinderer, G. Casula, O. Francis, H.-T. Hsu, Y. Imanishi, B. Meurers, J. Neumeyer, B. Richter, K. Shibuya, T. Sato, and T. Van Dam. 1999. Network of superconducting gravimeters benefits a number of disciplines. *EOS, Transactions, American Geophysical Union* 80: 121, 125–126.

Crossley, D., O. Jensen, and J. Hinderer. 1995. Effective barometric admittance and gravity residuals. *Physics of the Earth and Planetary Interiors* 90: 221–241.

Ferguson, J., T. Chen, J. Brady, C. Aiken, and J. Seibert. 2007. The 4D microgravity method for waterflood surveillance: Part II—Gravity measurements for the Pruhoe Bay reservoir, Alaska. *Geophysics* 72, no. 2: I33–I43.

Fredlund, D. 1976. Density and compressibility of air-water mixtures. *Canadian Geotechnical Journal* 13, 386–396.

Gehman, C.L., D.L. Harray, W.E. Sanford, J.D. Stednick, and N.A. Beckman. 2009. Estimating specific yield and storage change in an unconfined aquifer using temporal gravity surveys. *Water Resources Research* 45: W00D21. DOI: 10.1029/2007WR006096.

Goodkind, J.M. 1999. The superconducting gravimeter. *Review of Scientific Instruments* 70, no. 11: 4131–4152.

Hinderer, J., D. Crossley, and R. Warburton. 2007. Superconducting gravimeter. In *Treatise on Geophysics*, chap. 9, vol. 3, ed. T. Herring and G. Schubert. Boston, Massachusetts: Elsevier.

Hovorka, S.D., R. Mace, and E. Collins. 1998. Permeability structure of the Edwards Aquifer, South Texas—Implications for aquifer management. Report of Investigations, No. 250. Austin, Texas: Bureau of Economic Geology, University of Texas.

Hovorka, S.D., S. Rupple, A. Dutton, and J. Yeh. 1993. Edwards Aquifer Storage Assessment, Kinney County to Hays County, Texas. Contract Report to the Edwards Underground Water District, 101 p. Austin, Texas: Bureau of Economic Geology, University of Texas.

Hunt, B., B. Smith, S. Campbell, and S. Liang. 2004. Groundwater-Level Monitoring Program: Example from the Barton Springs Segment of the Edwards Aquifer, Central Texas. Texas Water Monitoring Congress. http://www.bseacd.org/uploads/AquiferScience/HR_Groundwater_Level%20Monitoring_TWMC_2004.pdf.

Jacob, T., R. Bayer, J. Chery, and N. LeMoigne. 2010. Time-lapse microgravity surveys reveal water storage heterogeneity of a karst aquifer. *Journal of Geophysical Research* 115: B06402. DOI: 10.1029/2009JB006616.

Kroner, C., and T. Jahr. 2006. Hydrological experiments around the superconducting gravimeter at Moxa Observatory. *Journal of Geodynamics* 41: 268–275.

Naujoks, M., A. Weise, C. Kroner, and T. Jahr. 2007. Detection of small hydrologic variations in gravity by repeated observations with relative gravimeters. *Journal of Geodesy* 82: 543–553. DOI: 10.1007/s00190-007-0202-9.

Pool, D. 2008. The utility of gravity and water-level monitoring at alluvial aquifer wells in southern Arizona. *Geophysics* 73: 49–59.

Pool, D., and J. Eychaner. Measurements of aquifer storage change and specific yield using gravity surveys. *Ground Water* 33, no. 3: 425–432.

Prothero, W., and J.M. Goodkind. 1968. A superconducting gravimeter. *Review of Scientific Instruments* 39: 1257–1262.

Rojstaczer, S., and D. Agnew. 1989. The influence of formation material properties on the response of water levels in wells to earth tides and atmospheric loading. *Journal of Geophysical Research* 94, no. B9: 12403–12411.

Rose, P.R. 1972. The Edwards Group, surface and subsurface, central Texas. Report of Investigations, No. 74, 198. Austin, Texas: Bureau of Economic Geology, University of Texas.

Scanlon, B., R. Mace, M. Barrett, and B. Smith. 2003. Can we simulate regional groundwater flow in a karst aquifer using equivalent porous media models? Case Study Barton Springs Segment, Edwards Aquifer. *Journal of Hydrology* 276: 137–158.

Senger, R., and C. Kreitler. 1984. Hydrogeology of the Edwards Aquifer, Austin Area, Central Texas. Report of Investigations, No. 35. Austin, Texas: Bureau of Economic Geology, University of Texas.

Smith, B., B. Hunt, and G. Schindel. 2005. Groundwater Flow in the Edwards Aquifer: Comparison of Groundwater Modeling and Die Tracer Tests. in Sinkholes and the Engineering and Environmental Impacts of Karst, American Society of Civil Engineers, Reston, Virginia.

Smith, B., and B. Hunt. 2004. Evaluation of sustainable yield of the Barton Springs Segment of the Edwards Aquifer, Hays and Travis Counties Central Texas. Report of the Barton Springs Edwards Aquifer Conservation District, 74p. Austin, Texas.

Van Camp, M., M. Vanclooster, O. Crommen, T. Petermans, K. Verbeeck, B. Meurers, T. van Dam, and A. Dassargues. 2006. Hydrogeological investigations at the Memback station, Belgium, and application to correct long periodic gravity variations. *Journal of Geophysical Research* 11: B10403. DOI: 10.1029/2006JB004405.

Van Camp, M., and P. Vauterin 2005. Tsoft: graphical and interactive software for the analysis of time series and Earth tides. *Computers & Geosciences* 31, no. 5: 631–640.

Wilson, C., H. Wu, L. Longuevergne, B. Scanlon, and J. Sharp. 2011. The Superconducting Gravimeter as a field Instrument applied to hydrology. In *International Association of Geodesy Symposium*, vol. 136, IAG2009. Berlin, Germany: Springer.

Wilson, C., B. Scanlon, H. Wu, J. Sharp, J. L. Longuevergne. 2008. *Turning a Superconducting Gravimeter into a Field Tool for Hydrological Studies, Colloquium CNFG2, Continental Water.* Paris, France: UNESCO.

Wilson, C., H. Wu, B. Scanlon, and J. Sharp. 2007. Taking the superconducting gravimeter to the field for hydrologic and other investigations. *EOS, Transactions, American Geophysical Union* 88, no. 53. Fall Meeting Supplement, Abstract H11A-050.